

Spin moment cancelation of high Curie temperature Ir doped ZrO_2 gradual atomic change

Z. Zarhri^{a,b,*}, O. Oubram^b, L. Cisneros Villalobos^b, and V. A. Leon Hernández^b

^aCONACYT-Faculty of Chemical Sciences and Engineering, The Autonomous University of the State of Morelos, Av. Universidad 1001, Col. Chamilpa, C.P. 62209, Cuernavaca, Morelos, Mexico.

^bFaculty of Chemical Sciences and Engineering, The Autonomous University of the State of Morelos, Av. Universidad 1001, Col. Chamilpa, C.P. 62209, Cuernavaca, Morelos, Mexico.

*e-mail: z.zarhri@gmail.com

Received 22 November 2022; accepted 20 January 2023

This paper presents the structural, magnetic properties, and spin moment cancelation phenomenon of the zirconium oxide with a gradual change of zirconium for Iridium. The density functional theory (DFT) is shown to be a key feature of magnetic properties of solid materials treatment. It's shown that a small adjustment of the spin moment (less than 6%) is allowed. The $Zr_{1-x}Ir_xO_2$ crystal structure deformation leads to a magnetic compensation which occurs at $x = 0.06$. Spin and orbital moments behaviors are discussed. The stability of the alloys compounds is confirmed by energy calculations. The material presents ferromagnetic stability and an indirect exchange coupling with a hybridization effect that permitted the evolution from a non-magnetic to a host material with magnetic properties. The Ir orbitals are set at the Fermi level and are spin polarized which indicates a half metallic behavior then makes the material a good candidate for spintronics' applications.

Keywords: DFT calculations; spin and orbital moment cancelation; Ir-doped ZrO_2 ; spintronics.

DOI: <https://doi.org/10.31349/RevMexFis.69.041601>

1. Introduction

Dilute magnetic semiconductors (DMS) [1] have been widely considered and still attracting much interest in the field of spintronic applications in the last decades [2,3], to find operational electronic materials with spin effect properties that can be obtained by atomic substitution or doping the host semiconductor with a magnetic element like Transition Metals (TM). These materials exhibit important properties among them the possibility to manipulate the electron charge as well as that of spin, which in turn can be used in spintronics applications to be used in quantum computers; [4-6] both in the use in spin-based polarized transistors and non-volatile RAMs [4]. And when doped with transition metal (TM), the dislocated magnetic moments can present ferromagnetic states at room temperature and good thermal equilibrium stability [7], which can give the possibilities of optimized spintronic' applications and devices. Several investigations were made these last years about doping diluted magnetic semiconductors and oxides like TiO_2 , SnO_2 , and ZrO_2 , to predict high-temperature ferromagnetism in some DMS, which gave these materials enormous interest concerning spintronic devices [8,9]. *E.g.*, spin-orbit interaction and the interface contribution of the spin-orbit coupling in such materials [10,11]. Zirconium dioxide (ZrO_2) has a wide band gap semiconductor with potential technological applications like gas sensors, solid fuel cells, high durability coating, and catalytic agents [12,13]. These make it a candidate in gate stack, dynamic access memory devices, and optical applications, thus, replacing SiO_2 as an advanced metal oxide semiconductor [14].

ZrO_2 is one of the ceramic materials with a large band gap and due to its suitable physical properties, is a good candidate for electronic and optoelectronic devices like red, blue, and green lasers and light-emitting diodes (LED), which are widely used for producing the full-color visible optical devices [15,16]. And its dielectric properties have diverse applications such as in gas sensors, solid fuel cells, high durability coating, and catalytic agents [14], in addition to possible uses due to its structural and optical characteristics in red, green, blue lasers, and light emitting diodes LED [17]. Previously in the study on the doping of Zirconium Dioxide with zirconium interstitial (Zr_i), antisite of zirconium (Zr_O), zirconium vacancy (VZr), oxygen interstitial (O_i), oxygen antisite (O_{Zr}), and oxygen vacancy (VO), it was shown that only oxygen interstitial (O_i), and oxygen antisite (O_{Zr}) provide magnetic moments in ZnO [14]. However, this paper presents the first principal calculations about pure ZrO_2 material, and the doping with Iridium element to show the effect of this non-TM defect on the magnetic properties of the zirconia. The phenomenon that leads to the magnetism in our material is discussed as also those responsible for the cancelation of the magnetic interactions at certain delocalized defect concentrations. The concentration variation of doping also is studied in this research paper to show the magnetic stability and estimate the Curie temperature of the compound.

2. Computational method and details

ZrO_2 has a cubic crystalline unit cell structure belonging to the space group number 216 Fm3m from the X-Ray Crys-

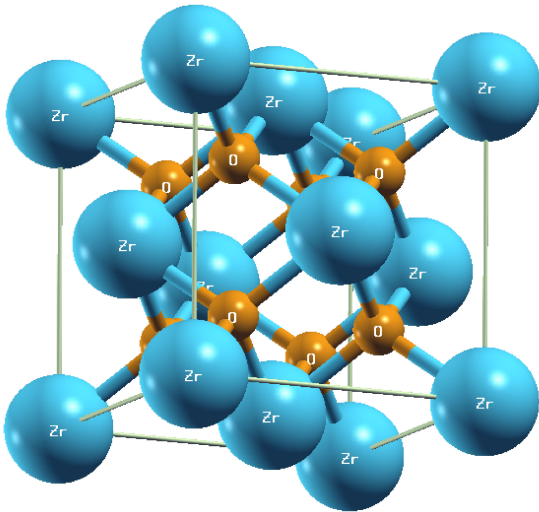


FIGURE 1. The unit cell of the Zirconium oxide ZrO_2 .

tallography international table, with a lattice parameter of 5.09\AA [18]. The inter-sites defects are represented by empty spheres $Z=0$. The atoms' positions are $4a$ Wyckoff $(0,0,0)$ for zirconium and $8c$ Wyckoff $(1/4,1/4,1/4)$ and $(3/4, 3/4,3/4)$ for the oxygen atoms. The zirconium oxide unit cell is presented in Fig. 1. The dislocated defects of Iridium are incorporated into the host material by atom change doping where Ir atoms replace Zr ones.

To study the ferromagnetism in the material alloy Ir-doped ZrO_2 , the density functional theory (DFT) was taken into consideration using the Korringa-Kohn-Rostoker (KKR) method implemented with the Coherent Potential Approximation (CPA) where the corresponding wave functions in the muffin-tin spheres may be expanded with the real harmonics up to $l = 2$, where l is the angular momentum defined at different sites. The Local Density Approximation (LDA) is one of the most used approximations to calculate the exchange and correlation potential with a slow fluctuation of the electron density. Thus, this approximation allows the replacement of the exchange-correlation term at each point with that of a uniform gas of interacting electrons which allows high precision in the results [19,20]. The KKR-CPA and the Green functions implemented in the MACHIKANEYAMA electronic structure calculation code [21] used in the present work are effective for studying the electronic properties of disordered systems such as alloys because it takes into account (as described by Friedel fourteen years earlier [20]), the influence on electrical conduction of the hybridization of the $s - p$ bands with the d bands as well as of the virtual bound states.

3. Results and discussion

The density of states of our pure and Ir-doped ZrO_2 was investigated to examine the electronic structure and the magnetism in the above-mentioned alloy. The oxygen atoms around Zr ones form a crystal field that allows the $3d$ zir-

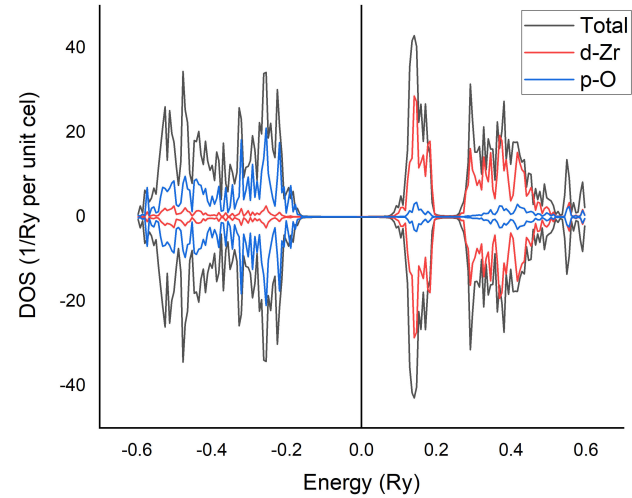


FIGURE 2. The total and partial densities of states of Pure ZrO_2 .

conium orbitals to be split to $t2g$ and eg successively upper triply degenerate and lower doubly degenerate [22].

The total and partial density of states of pure zirconium oxide shown in Fig. 2 indicate a non-magnetic material due to the symmetry between minority and majority spins in up and down states of orbitals in both valence and conduction bands [23]. This is confirmed by a zero magnetic moment computed for this material. A notable underestimation of the band gap value found (about 3.01 eV) compared to the experimental results of 5.7 eV [24], is due to the overestimation of the interaction energy by the DFT method [25]. This can be observed in the figure where the valence band has a large width, with a main contribution of the oxygen p orbital while the zirconium d orbitals are mainly located at the conduction band. It was previously demonstrated that defects induce states in the band gap where its locations concerning the valence band maximum conduction band minimum can help predict the contribution of the dislocated atoms and their different magnetic aspects [26,27].

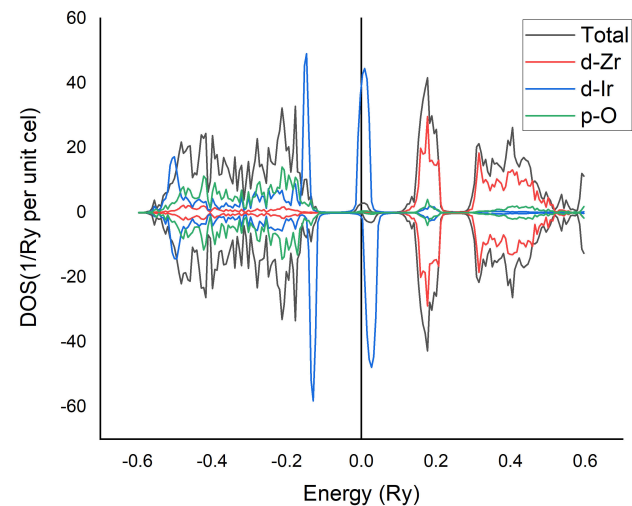


FIGURE 3. The total and partial densities of states of Iridium doped ZrO_2 at 3%.

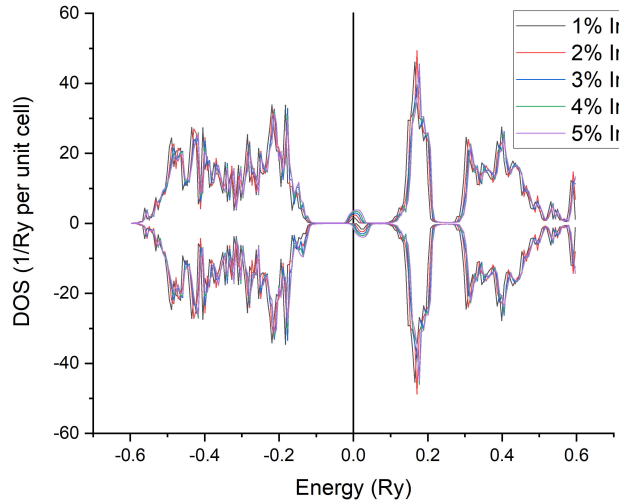
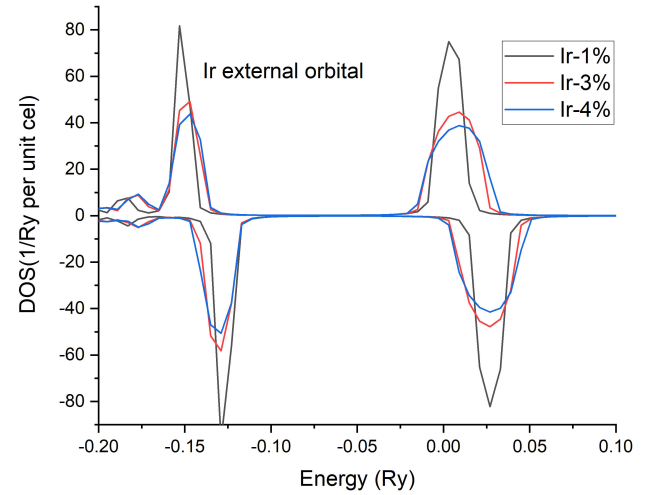


FIGURE 4. The total DOS evolution with Ir doping variation.

From Fig. 3, which presents the total and partial densities of states of ZrO₂ doped with Ir at 3% of Zr atom change, we can observe an Ir band located at the Fermi level. This Ir(3*d*) spin polarization has a third party in the valence band and the rest in the conduction band. This means that it's a *t*2*g*+ orbital containing one electron which gave the material a half-metallic behavior. The *eg* orbitals (*eg*+ and *eg*-) are completely occupied and located in the valence band, while the *t*2*g*- is empty and located in the valence band [28]. In the valence band, we can notice a notable contribution of the oxygen *p* orbital atoms which is due to their interaction with the new Ir dislocated defect. This hybridization of oxygen with iridium atoms gave rise to magnetism in the material due to the exchange atomic coupling [29]. The non-zero magnetic moment of the new alloys confirms that the material is a diluted magnetic semiconductor.

Figure 4 shows an evolution of the density of states of the compound as a function of Ir atoms doping. It can be noticed a small shift of the valence band to higher energy indicates that the doping elements introduce new partially occupied states in the band gap with the creation of new positive charge carriers allowing the excitation of electrons from the valence to the conduction band and then making the Ir-doped ZrO₂ and acceptor. The indirect coupling exchange character in this material is because of the intervention of the oxygen


 FIGURE 5. The double exchange coupling and Ir-*d* orbital behavior.

atoms in the magnetic interaction between localized magnetic moments carried by iridium charge carriers [30]. This also led to a ferromagnetic aspect due to the exchange splitting of Ir(3*d*) orbitals with a large variation that could lead to a high tunnel barrier and then produce a spin-polarized current. This ferromagnetic behavior is verified by an energy stability comparison between the ferromagnetic state and a disordered local state created by splitting half of the spins to simulate an anti-ferromagnetic magnetic moment [27,31].

There is a hybridization between the oxygen and the iridium bands that indicates an indirect coupling. And due to the enlargement and the amplitude reduction of the Ir-*d* orbital peaks shown in Fig. 5, it can be concluded that the magnetic interaction has a double exchange behavior [32]. Table I shows the variation of the total energy, total magnetic moment, and partial magnetic moments of Zr, Ir, and O. It can be seen that the total magnetic moment increases by increasing the amount of the iridium impurities till it reaches 6% of Ir where it suddenly decreases then disappear at 7% or more. This may be due to the solubility of the material and its structural changes because of the atomic radius difference between Ir and Zr where the atomic radius of Ir = 0.2 nm and the one of Zr = 0.160 nm. This phenomenon of spin moment

TABLE I. The variation of the total energy and the total and partial spin moment as a function of the Ir doping concentration.

	Total Energy	Total magnetic moment	Zr spin moment	Oxygen spin moment	Ir spin moment
Pure	-7489.2214621	0	0	0	
Ir at 1%	-7649.5048476	0.0128	0.00053	0.00177	0.74409
Ir at 2%	-7914.9012634	0.0225	0.00089	0.00318	0.65074
Ir at 3%	-8180.2977255	0.0317	0.00123	0.00451	0.61039
Ir at 4%	-8445.6942096	0.0402	0.00154	0.00574	0.58167
Ir at 5%	-8711.0907072	0.0443	0.00167	0.00633	0.51290
Ir at 6%	-8976.4847222	0.0184	0.00070	0.00263	0.17854

cancelation due to a non-collinear magnetic arrangement produces a deformation of the structure of Ir-doped ZrO_2 and changes the interaction distance of the polaron of delocalized and localized spins [33], thus reducing the magnetic interactions and then the magnetic moment till its annulation.

The existence of the oxygen spin moment indicates the indirect interaction and the contribution of the oxygen in the magnetic interactions. Its variation is also increasing with the Ir concentration till the cancelation of spin and orbital moments [34]. The increase in the magnetic moment of Zr and the decrease in the magnetic moment of Ir are due to the phenomenon of magnetic moment compensation that leads to an average interaction between different spins [35]. The Ferromagnetic state is the lowest in energy consideration. With Ir atom doped compounds, the energy difference is going to be smaller and still dominates the Ferromagnetic states. The local spin moment per Ir atom seems to decrease which increases the O and Zr spin moment, whereas the net magnetic moment of a doped compound increases gradually till 5% of the impurity concentrations. The ferromagnetic stable state is confirmed by comparing the energy of the ferromagnetic and the Disordered Local Moment state "DLM", which is simulated by splitting the spin carriers and applying a successively UP and DOWN polarization of each half of them, then calculating the total energy of each system. The Ferromagnetic state shows lower total energy compared to the DLM one, which makes it more stable. This allows us to estimate the magnetic phase change Curie temperature using the Mean Field Approximation and the following equation [36]: can be introduced as numbered equations

$$K_B T_C = \frac{3 \Delta E}{2 c}, \quad (1)$$

where K_B is the Boltzmann constant, T_C is the Curie temperature, ΔE is the energy difference between the DLM state

and the ferromagnetic state, C is the Concentration of the Ir atoms.

The results are 301 K for 1% atomic change Ir doping, then goes decreasing, this makes the material a good candidate for spintronics and optoelectronics applications with an energetically stable structure in comparison with the pure host material indicated by the lower total energy values found [37].

4. Conclusion

DFT was used to study the electronic structure and predict the structural, electronic, and magnetic properties of zirconium oxide with a gradual atomic change of Zr by Iridium atoms. The material presents a high Curie temperature at a low concentration of the doping element. The gradual zirconium change allows the adjustment of the material spin moment until 6% of iridium. Then a complete spin and orbital moment cancelation phenomenon appears at 7% due to a non-collinear magnetic arrangement caused by Ir and its radius difference that leads to structural deformation. The magnetic interaction in this material is a double exchange type because of the indirect coupling with the oxygen atoms. The iridium $t2g+$ orbital is partially occupied which makes it located at the Fermi level with a 100% spin-polarized. This makes the material have a half-metallic behavior, thus making it a good candidate for spintronics and optoelectronics applications.

Acknowledgments

The authors would like to send a special thanks to the CONACYT-Mexico project Investigadores por Mexico - CONACYT number CIR/0065/2022, also to the National Laboratory of Supercomputers project LNS202101008N and finally to CONACYT - Fronteras project CF19-2096029, Mexico for the financial support.

1. C. Klingshirm, Introduction to semiconductor quantum structures: Semiconductor Quantum Structures, Growth and Structuring (2013) 1, https://doi.org/10.1007/978-3-540-68357-5_1.
2. A. Hirohata *et al.*, Review on spintronics: Principles and device applications, *Journal of Magnetism and Magnetic Materials* **509** (2020) 166711, <https://doi.org/10.1016/j.jmmm.2020.166711>.
3. Z. Mahdaviifar and F. Shojaei, CdInGaS4: An unexplored twodimensional materials with desirable band gap for optoelectronic devices, *Journal of Alloys and Compounds* **854** (2021) 157220, <https://doi.org/10.1016/j.jallcom.2020.157220>.
4. Z. Zarhri *et al.*, Ab-initio study of magnetism behavior in TiO2 semiconductor with structural defects, *Journal of Magnetism and Magnetic Materials* **406** (2016) 212, <https://doi.org/10.1016/j.jmmm.2016.01.029>.
5. M. Plonus, Electronics and communications for scientists and engineers (Butterworth-Heinemann, 2020), <https://doi.org/10.1016/C2018-0-00442-9>.
6. D. Shi, Nanomaterials and devices (Elsevier, 2014), <https://doi.org/10.1016/C2012-0-03204-8>.
7. Z. Zarhri *et al.*, Magnetic properties of transition metal-doped CdSe, *Journal of Superconductivity and Novel Magnetism* **28** (2015) 2155, <https://doi.org/10.1007/s10948-015-2986-9>.
8. S. Pearton *et al.*, Ferromagnetism in transition-metal doped ZnO, *Journal of Electronic Materials* **36** (2007) 462, [https://doi.org/10.1016/S1386-9477\(01\)00093-5](https://doi.org/10.1016/S1386-9477(01)00093-5).
9. T. Fukumura, H. Toyosaki, and Y. Yamada, Magnetic oxide semiconductors, *Semiconductor Science and Technology* **20** (2005) S103, https://doi.org/10.1007/978-94-007-6892-5_22.

10. Z. A. Devizorova *et al.*, Interface contributions to the spin-orbit interaction parameters of electrons at the (001) GaAs/AlGaAs interface, *JETP letters* **100** (2014) 102, <https://doi.org/10.1134/S0021364014140033>.
11. U. C. Mendes *et al.*, Electronic and optical properties of InGaAs quantum wells with Mn-delta-doping GaAs barriers, arXiv preprint arXiv:1509.07136 (2015), <https://doi.org/10.48550/arXiv.1509.07136>.
12. S. A. Steiner III *et al.*, Nanoscale zirconia as a nonmetallic catalyst for graphitization of carbon and growth of single- and multiwall carbon nanotubes, *Journal of the American Chemical Society* **131** (2009) 12144, <https://doi.org/10.1021/ja902913r>.
13. Z. Xiao *et al.*, Materials development and potential applications of transparent ceramics: A review, *Materials Science and Engineering: R: Reports* **139** (2020) 100518, <https://doi.org/10.1016/j.mser.2019.100518>.
14. M. Boujnah *et al.*, Magnetic and electronic properties of point defects in ZrO₂, *Journal of superconductivity and novel magnetism* **26** (2013) 2429, <https://doi.org/10.1007/s10948-012-1826-4>.
15. L. Zeng *et al.*, Molecular beam epitaxial growth of lattice-matched ZnxCdyMg1-x-ySe quaternaries on InP substrates, *Journal of crystal growth* **175** (1997) 541, [https://doi.org/10.1016/S0022-0248\(96\)00873-1](https://doi.org/10.1016/S0022-0248(96)00873-1).
16. P. Huang *et al.*, Photoluminescence and contactless electroreflectance characterization of BexCd1-xSe alloys, *Journal of Physics: Condensed Matter* **19** (2006) 026208, <https://doi.org/10.1088/0953-8984/19/2/026208>.
17. H. Masui and S. Nakamura, White Light-emitting Diodes, *Encyclopedia of Materials: Science and Technology* (2010).
18. E. Stefanovich, A. L. Shluger, and C. Catlow, Theoretical study of the stabilization of cubic-phase ZrO₂ by impurities, *Physical Review B* **49** (1994) 11560, <https://doi.org/10.1103/physrevb.49.11560>.
19. Y. Ziat *et al.*, Computational study of the magnetic and electronic properties of the LiMgN (Vcl-xZx) and LiMg (N1-xZx) alloys where Z is B, C or S, *Computational Condensed Matter* **25** (2020) e00502, <https://doi.org/10.1016/j.cocom.2020.e00502>.
20. M. Saint-Cricq, Modélisation des coefficients de transport thermoélectriques des alliages métalliques multicomposants, Ph.D. thesis, Université Grenoble Alpes (2020).
21. Y. Ziat *et al.*, Ferrimagnetism and ferromagnetism behavior in (C, Mn) co-doped SnO₂ for microwave and spintronic: Ab initio investigation, *Journal of Magnetism and Magnetic Materials* **483** (2019) 219, <https://doi.org/10.1016/j.jmmm.2019.03.084>.
22. E. Grządka and J. Matusiak, Changes in the CMC/ZrO₂ system properties in the presence of hydrocarbon, fluorocarbon and silicone surfactants, *Journal of Molecular Liquids* **303** (2020) 112699, <https://doi.org/10.1016/j.molliq.2020.112699>.
23. I. Kuryliszyn-Kudelska *et al.*, Adjusting the magnetic properties of ZrO₂: Mn nanocrystals by changing hydrothermal synthesis conditions, *Magnetochemistry* **4** (2018) 28, <https://doi.org/10.3390/magnetochemistry4020028>.
24. F. Gallino, C. Di Valentin, and G. Pacchioni, Band gap engineering of bulk ZrO₂ by Ti doping, *Physical Chemistry Chemical Physics* **13** (2011) 17667, <https://doi.org/10.1039/C1CP21987A>.
25. P. Borlido *et al.*, Exchange-correlation functionals for band gaps of solids: benchmark, reparametrization and machine learning, *npj Computational Materials* **6** (2020) 96, <https://doi.org/10.1038/s41524-020-00360-0>.
26. F. A. Kröger and N. H. Nachtrieb, The chemistry of imperfect crystals, *Physics Today* **17** (1964) 66, <https://doi.org/10.1063/1.3051186>.
27. Z. Zarhri *et al.*, Titanium atoms dimerization phenomenon and magnetic properties of titanium-antite (TiO) and chromium doped rutile TiO₂, ab-initio calculation, *Journal of Physics and Chemistry of Solids* **94** (2016) 12, <https://doi.org/10.1016/j.jpcs.2016.03.002>.
28. Z. Zarhri, A. Benyoussef, and A. El Kenz, Theoretical study of TiO₂ doped with single and double impurities, *Journal of Superconductivity and Novel Magnetism* **27** (2014) 1323, <https://doi.org/10.1007/s10948-013-2439-2>.
29. C. Lin *et al.*, Hybridization effects-The evolution from nonmagnetic to magnetic behavior in uranium-based systems, *Journal of the Less Common Metals* **133** (1987) 67, [https://doi.org/10.1016/0022-5088\(87\)90461-9](https://doi.org/10.1016/0022-5088(87)90461-9).
30. E. Coronado, B. Tsukerblat, and R. Georges, Exchange interactions I: mechanisms, *Molecular magnetism: from molecular assemblies to the devices* (1996) 65, https://doi.org/10.1007/978-94-017-2319-0_3.
31. Y. Ziat *et al.*, First-Principles Study of Magnetic and Electronic Properties of Fluorine-Doped Sn_{0.98}Mn_{0.02}O₂ System, *Journal of Superconductivity and Novel Magnetism* **29** (2016) 2979, <https://doi.org/10.1007/s10948-016-3609-9>.
32. G. Gao *et al.*, Half-metallic ferromagnetism of Cr-doped rutile TiO₂: A first-principles pseudopotential study, *Physica B: Condensed Matter* **382** (2006) 14, <https://doi.org/10.1016/j.physb.2006.01.501>.
33. R. Wood, Spin-polarons and high-T_c superconductivity, Tech. rep., Oak Ridge National Lab., TN (United States) (1994), <https://doi.org/10.2172/10158128>.
34. P. Söderlind, Cancellation of spin and orbital magnetic moments in δ-Pu: Theory, *Journal of alloys and compounds* **444** (2007) 93, <https://doi.org/10.1016/j.jallcom.2006.10.084>.
35. A. Iyushin *et al.*, The phenomenon of magnetic compensation in the multi-component compounds (Tb, Y, Sm) Fe₂ and their hydrides, *Journal of Alloys and Compounds* **847** (2020) 155976, <https://doi.org/10.1016/j.jallcom.2020.155976>.
36. M. Shahjahan, I. Razzakul, and M. Rahman, First-principles calculation of stable magnetic state and Curie temperature in transition metal doped III-V semiconductors, *Computational Condensed Matter* **9** (2016) 67, <https://doi.org/10.1016/j.cocom.2016.10.001>.
37. M. Morinaga, H. Adachi, and M. Tsukada, Electronic structure and phase stability of ZrO₂, *Journal of Physics and Chemistry of Solids* **44** (1983) 301, [https://doi.org/10.1016/0022-3697\(83\)90098-7](https://doi.org/10.1016/0022-3697(83)90098-7).